Title	Self-consistent band structure, Fermi surface, and magnetic ordering in europium
Sub Title	
Author	福地, 充(Fukuchi, Mitsuru) 松本, 紳(Matsumoto, Makoto) 小林, 正一(Kobayashi, Shoichi) Sakiji, Yukihiro
Publisher	慶應義塾大学理工学部
Publication year	1984
Jtitle	Keio Science and Technology Reports Vol.37, No.1 (1984. 5) ,p.1- 11
JaLC DOI	
Abstract	The energy band structure of Eu was calculated by using the self-consistent KKR method. Our band structure shows excellent agreement with the optical data of Endriz and Spicer. The Fermi surface topology, the helical spin ordering in bcc Eu at low temperatures, and the de Haas-van Alphen frequencies for some magnetic field directions are discussed.
Notes	
Genre	Departmental Bulletin Paper
URL	https://koara.lib.keio.ac.jp/xoonips/modules/xoonips/detail.php?koara_id=KO50001004-00370001-0001

KEIO SCIENCE AND TECHNOLOGY REPORTS
VOL. 37, NO. 1, pp. 1-11, 1984

SELF-CONSISTENT BAND STRUCTURE, FERMI SURFACE, AND MAGNETIC ORDERING IN EUROPIUM

Mitsuru FUKUCHI, Makoto MATSUMOTO,

**Department of Instrumentation Engineering,
Faculty of Science and Technology,
Keio University,
Hiyoshi-3, Yokohama 223, Japan**

Syo-Iti KOBAYASI and Yukihiro SAKIZI

**Physics Department, Nihon University, Sakurajosui-3,
Setagaya-ku, Tokyo 156, Japan**

(Received February 22, 1984)

ABSTRACT

The energy band structure of Eu was calculated by using the self-consistent KKR method. Our band structure shows excellent agreement with the optical data of Endriz and Spicer. The Fermi surface topology, the helical spin ordering in bcc Eu at low temperatures, and the de Haas-van Alphen frequencies for some magnetic field directions are discussed.

§1. Introduction

Europium is located at the center of the 15 rare-earth (RE) elements in the periodic table and is the only RE-metal which shows bcc structure in the ordinary temperature and pressure range. Eu is also unique and interesting in that, although normally the RE's are trivalent, this metal is divalent with a half-filled symmetric 4f-shell, and moreover it is known to have a helical magnetic ordering below the Néel temperature $T_N=91$ K with a spin rotation axis in the [001]-direction.[1]

The energy bands of Eu have been calculated by Freeman and Dimmock,[2] Andersen and Loucks[3] (hereafter referred to as AL), Kobayasi, Fukuchi and Nagai[4] (KFN), and Matsumoto, Shibata, Sakizi, Fukuchi and Kobayasi.[5] Especially, the paper by AL is significant in that the details of the Fermi surface of bcc Eu were shown for the first time and the occurrence of a noncommensurate periodic moment arrangement in this metal was discussed.

None of the earlier calculations were self-consistent. With this in mind, we have made a self-consistent calculation of the band structure of Eu. In a separate paper discussing the density of states and isomer shift, it has been shown[6] that the Fermi energy E_F ($=0.271_3$ Ryd) is located near the dip of the density of states

curve. The coefficient of the electronic contribution to the heat capacity and the contribution to the isomer shift of Eu^{151}-nucleus have been reported.[6]

The plan of this paper is as follows. In Sec. 2 we outline our procedure for the self-consistent calculation. In Sec. 3 the relationship between the calculated Fermi surface topology and the experimentally observed helical arrangement of magnetic moments is discussed. In Sec. 4 we compare our SCF-band structure with the optical data of Endriz and Spicer.[7] The results of calculated dHvA-frequencies are reported in some detail in Sec. 5. We discuss in Sec. 6, the expected changes caused by relativistic effects on our band structure.

§2. Procedure

For the crystal potential we employ the usual muffin-tin shape with Slater's $X\alpha$-type local exchange potential. We have done two SCF calculations with $\alpha=1.0$ and $\alpha=2/3$. We assume the electron-configuration of bcc Eu as (Xenon-core) $(4f)^7$ $(CE)^2$, where CE means conduction electrons. For the Xenon-core wave-functions, we calculated the SCF atomic orbitals for $\alpha=1.0$ and for $\alpha=2/3$ using a Herman-Skillman's method.[8] Although relativistic effects play important roles for heavier atoms as rare earth elements, we have started from the non-relativistic solutions for Xe-core functions. These have been used throughout our present calculations for the reason given in the following paragraph.

In the process of calculating the isomer shift on a Eu^{151}-nucleus,[9] we have established that the contribution from the 5s-shell electrons to the density at the nucleus is practically unchanged in Eu metal and Eu^{2+}-compounds, although the 5s eigenvalues for both crystals differ from each other by more than 1 Ryd. Based on this fact, we suppose that the space behavior of the 5s- and 5p- and more inner shell-electron wave-functions remain practically unchanged in Eu metal in the course of the self-consistent procedure. The number of 4f-electrons are kept fixed at seven throughout the SCF process.

On the other hand, the outer-electron parts $(4f)^7$ $(CE)^2$ are made self-consistent in our present calculation. Since we do not take into account the exchange polarization,[10] the crystal charge density $\rho_{crys}(r)$ is written as

$$\rho_{crys}(r)=\rho_{\uparrow crys}(r)+\rho_{\downarrow crys}(r)=2\rho_{\uparrow crys}(r)\ , \tag{1}$$

where $\uparrow$ and $\downarrow$ denote the contribution of the up- and down-spin electrons. In this paper we concentrate on the $\alpha=1.0$ results since the conduction band widths seem to give better agreement with optical experiments. We have done the SCF calculations for the valence electrons both $\alpha=1.0$ and 2/3 crystal potentials. The $\alpha=1.0$ calculations place the 4f levels below the conduction bands and $\alpha=2/3$ ones place the 4f levels in the middle part of the occupied conduction bands. On one hand, optical measurements do indicate that the position of the occupied 4f states is below the conduction bands.[7] Therefore we have chosen $\alpha=1.0$ potential as SCF potential for Eu metal. The position of the 4f states is, however, very sensitive to approximations in the potential and cannot reliably be determined by band structure methods. The final decision of α-value seems to the remained problem for us.

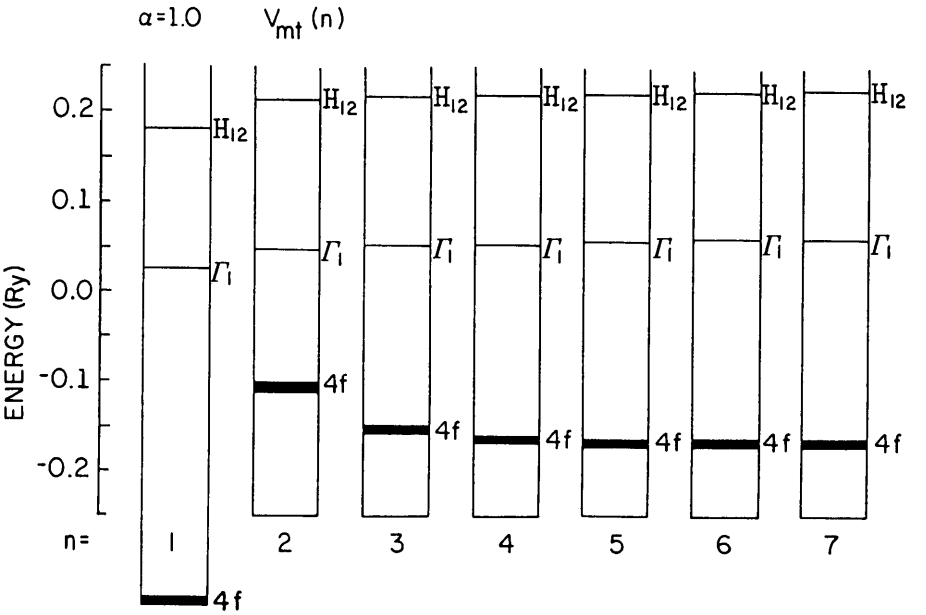

Figure 1. Convergence of Γ_1-, H_{12}-, and 4f-states in seven iterations.

Now, we find that seven iterations are sufficient to achieve convergence under the criterion that the 4f eigen-values change by less than 0.5% between iterations. The energy level positions of Γ_1 and H_{12} are almost unchanged throughout the iteration process as shown in Fig. 1. The 4f bands are located at 3.1$_3$ eV below the bottom of the conduction bands.

Next, although there are many evidences that the relativistic effects are important in heavier elements such as rare earths (in fact, AL have made RAPW-calculation for Eu), we have not included those effects in the present calculations. We will discuss this point later.

§3. Fermi Surface and Helical Spin Ordering

As is reported by AL and KFN, the Fermi surface of bcc Eu consists of two parts: the electron surface around H-point and the hole surface around P-point (Fig. 2). The two pieces of the Fermi surface were named by AL as follows. The holes at P were called the "tetracube", as they were shaped like a rounded-off cube with ellipsoids tetrahedrally positioned on four of the corners. Similarly, the electrons at H were shaped like a rounded-off cube, and AL called this surface the "superegg".

The results of KFN were fairly similar, in general, to those of AL, particularly in the shape of the hole surface. But here was a significant difference in the shape of the electron Fermi surface: KFN's electron surface was "nearly spherical",

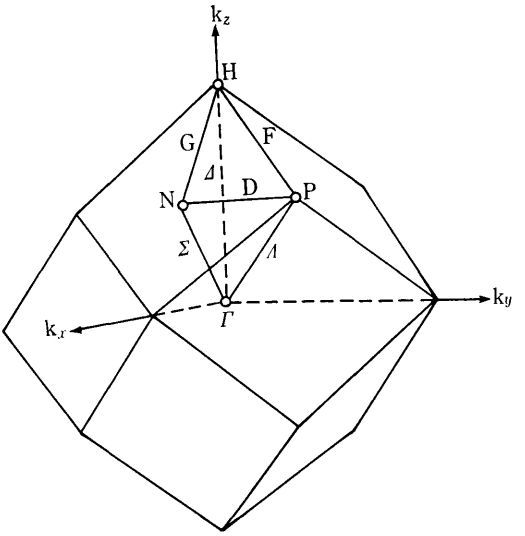

Figure 2. bcc Brillouin zone and its 1/48.

although AL's electron surface was "nearly cubic".

Now, in order to investigate this point more thoroughly, we performed a self-consistent band calculation. The electron and the hole Fermi surfaces obtained in the present calculation are shown in Figs. 3 (a) and (b), respectively. Our Fig. 3 (b) resembles quite clearly AL's "tetracube". Now, as is well known, the "nesting" portions of the Fermi surface determine the wave vector $\boldsymbol{Q}$ of helical spin ordering. As AL have pointed out, it is clear that the $\boldsymbol{Q}$ in europium is in the [001]-direction and this $\boldsymbol{Q}$ is fixed by the nesting of the opposed nearly cubical pieces of the hole Fermi surface (tetracube). The experimental value of the $\boldsymbol{Q}$ by Nereson, Olsen and Arnold[1] (NOA) was 0.209 a.u. (atomic units), and was almost temperature-independent. The distance between the faces of the tetracube by AL was 0.238 a.u., and KFN's value was 0.240 a.u.. The present value of $\boldsymbol{Q}$ is 0.254 a.u. which is not much different from the earlier calculations and is in fairly good agreement with (but a little larger than) the experimental one.

Next, we turn to discuss the role of the electron Fermi surface. AL's electron surface (superegg) was itself a rounded-off cube and the parallel faces are separated by almost exactly twice the wave vector of the helical spin ordering. Then, AL discussed that the first-order contribution from the superegg will produce a second maximum in susceptibility at $\boldsymbol{q}=2\boldsymbol{Q}$, and the second-order contribution will help in holding a maximum at $\boldsymbol{q}=\boldsymbol{Q}$.

Now, our electron Fermi surface ("bumpy sphere") resembles a sphere around H as shown in Fig. 3 (a), and therefore, there are no significant nesting portions in [001]-direction or in any other directions. Thus, it seems that we do not expect any contribution from the electron Fermi surface to the "nesting". We note that our present results of both the electron and the hole Fermi surfaces may be considered to be consistent with the neutron diffraction results of NOA.[1]

§4. Comparison with the Optical Experiment

Endriz and Spicer[7] have made reflectance measurements on the isoelectronic divalent bcc metals Eu and Ba in parallel, and obtained the experimental spectrum of interband optical conductivity $\sigma(\omega)$, which is shown in Fig. 4 (b). Here the abscissa is normalized to the free electron plasma energy which for Eu is $\hbar\omega_p=$

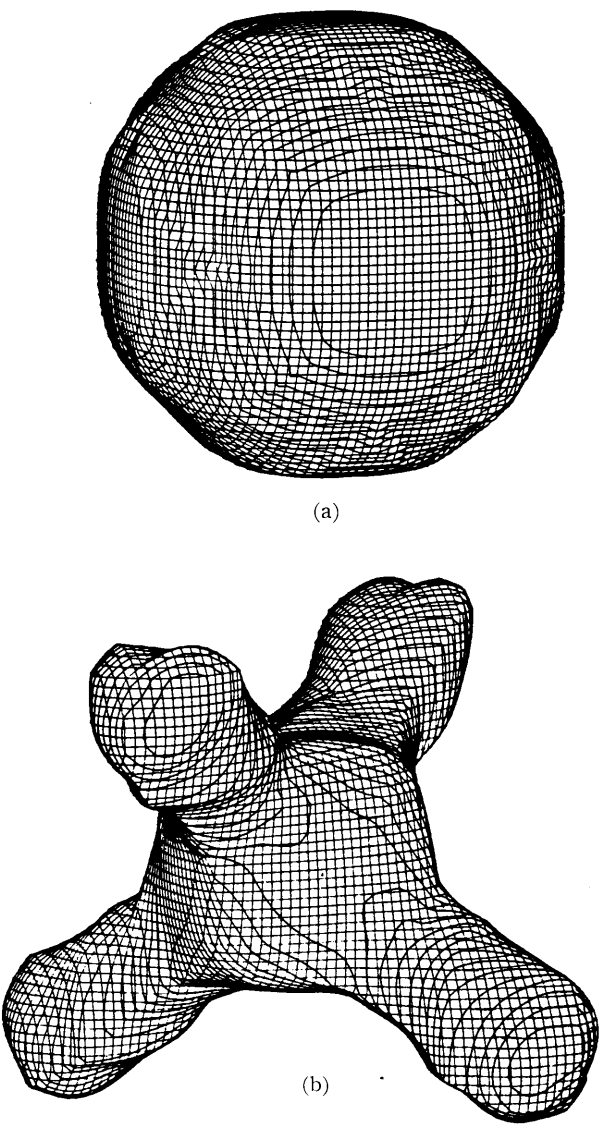

Figure 3. Fermi surface obtained in the present SCF-band calculation. (a) Electron Fermi surface ("bumpy sphere"). (b) Hole Fermi surface ("tetracube").

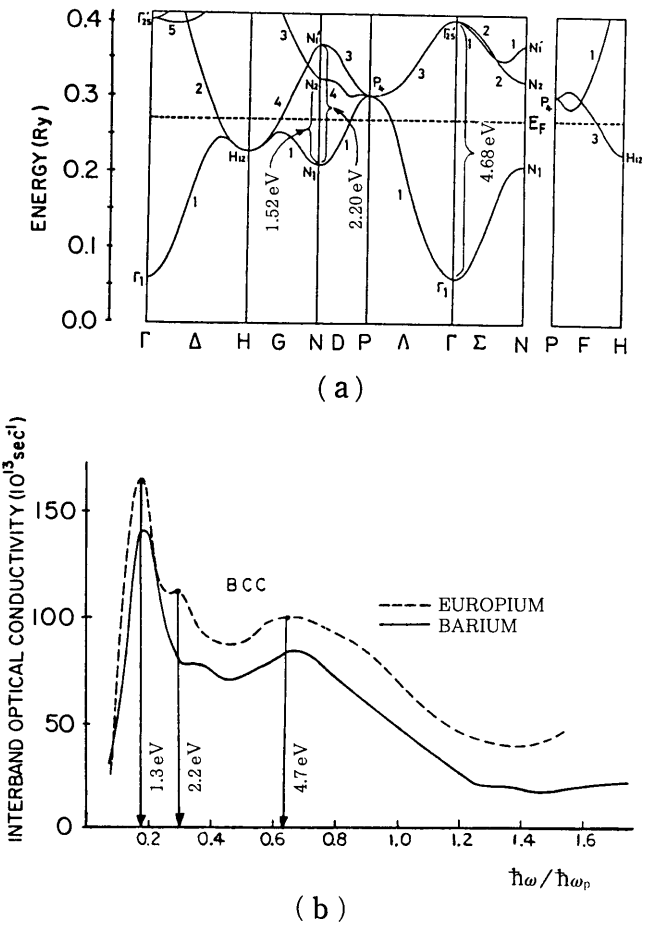

Figure 4. Comparison of the present SCF-bands and the optical data of Ref. 7.

7.57 eV. Endriz and Spicer compared their experimentally determined peak positions with the results of the band calculation of Eu made by Freeman and Dimmock,[2] and they obtained fairly good agreement.

Now, our present SCF-band structure along the symmetry axes is shown in Fig. 4 (a), where we have indicated our tentative assignment of the three major critical point structures in the experimental $\sigma(\omega)$, Fig. 4 (b). The agreement is excellent, except for the first peak where the agreement is only fair. The first peak may correspond to transitions from N_1 which has the character of s- and d-states to N_2 which is a pure d-state. Although this transition is dipole forbidden the neighboring points near N_1 have s-, p- and d-character, and similarly many points near N_2 have p- and d-character, so that the transitions near these points are not forbidden. Next, the second peak corresponds to transitions from the same N_1 to the higher state N_1' which has p-character, and there is no matrix element problem for the transition. The value of the third transition is agreement with

the Γ'_1-Γ'_{25} energy-eigenvalue, from Γ'_1 which is a pure s-state to Γ'_{25} which is a pure d-state, but again points near Γ'_1 have s-, p- and d-properties, and points near Γ'_{25} have p- and d-character, therefore transitions in the neighborhood of Γ'_1 are not forbidden. The density of states of near the Γ'_1 state, however, is exceedingly small, so it seems that this transition hardly contribute to the optical measurement. Preferably, we think that the higher bands mainly contribute to the third transition peak in Fig. 4 (b). But, of course, in order to explain the experimental intensity, it is necessary to compute the matrix elements of transition probability, and in addition, we would have to calculate the band structure up to a higher energy region. We are computing the generalized susceptibility and the joint density of states to elucidate this point and in near future, these results will be discussed in other paper.

§5. de Haas-van Alphen Frequencies Computed by Our Fermi Surfaces

As mentioned above, the Fermi surface of bcc Eu consists of the electron surface around the H-point and the hole surface around the P-point. The projections of the electron Fermi surface in a plane perpendicular to the [001]-directions are shown in Fig. 5 for various values of k_z (measured along [001]), and those of the hole Fermi surface perpendicular to the [111]-direction are in Fig. 6.

Extremal cross-sections in $\boldsymbol{k}$-space perpendicular to [001]-, [011]- and [111]-directions for both the electron and the hole Fermi surfaces are shown in Figs. 7 (a) and (b), respectively. The extremal areas for the electron Fermi surface are

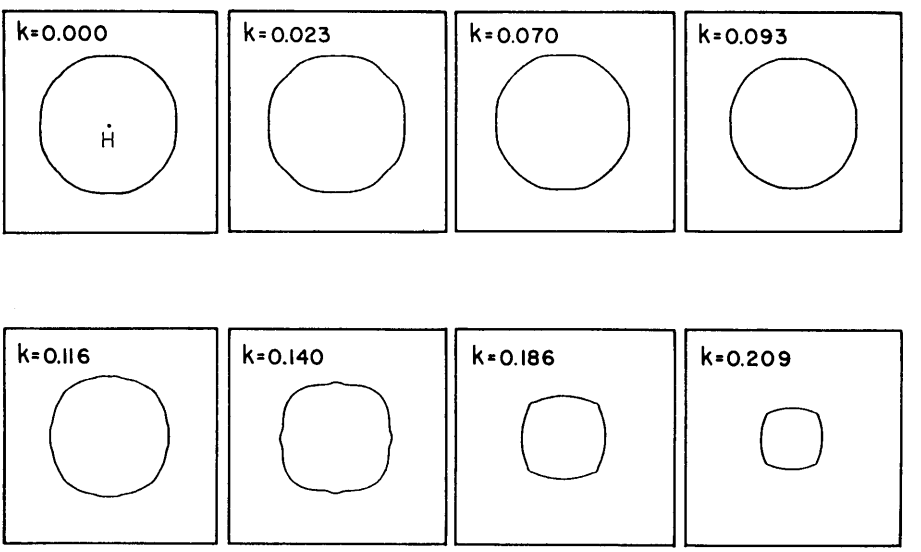

Figure 5. Shapes of cross-sections of our "bumpy sphere" perpendicular to the [001]-direction.

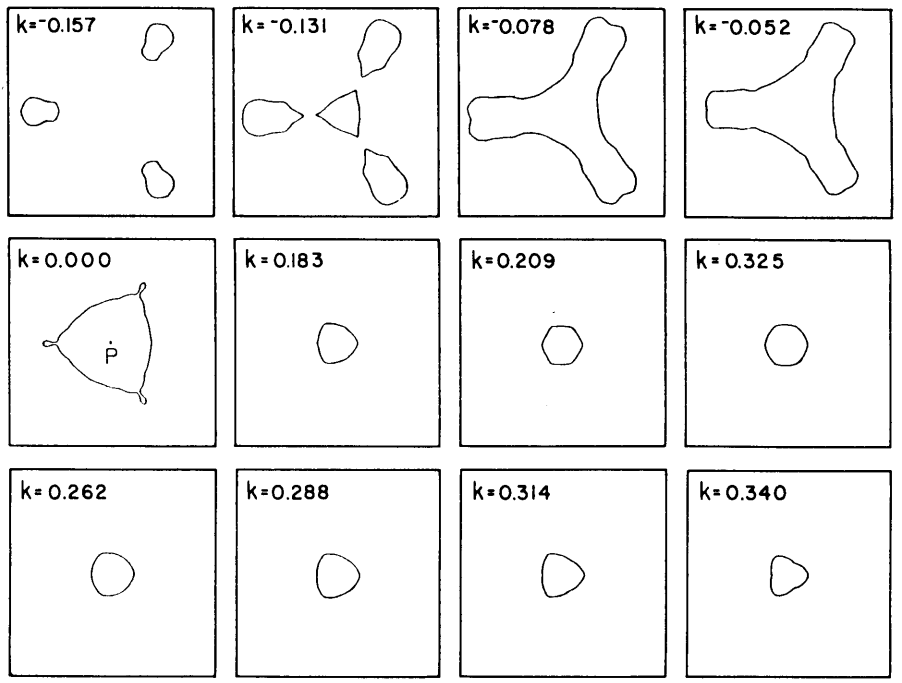

Figure 6. Shapes of cross-sections of our "tetracube" perpendicular to the [111]-direction.

obtained in each direction at the plane through H-point, and their numerical values are given in Fig. 7 (a). We note that these three values are almost equal to each other, which shows that the electron Fermi surface around H is nearly a sphere. On the other hand, the extremal cross-section areas for the tetracube are more complicated than for the electron Fermi surface, as shown in Fig. 7 (b). In the [111]-direction, we have a shallow minimum and a shallow maximum in areas on the tetracube arm, and another large maximum area due to the tetracube body. In the [001]- and [011]-directions, the cross-section areas are symmetric around the P-point. In the [011]-direction, two shallow maximum and two shallow minimum areas and a large maximum one through the P-point are found. In the [001]-direction, one minimum (through P) and two maximum (on both sides of P) areas are obtained. The results of our present calculation are summarized in Table 1.

We list these frequencies for the sake of comparison with those given by AL for their paramagnetic calculations, and also for use as a reference for when calculations or experiments are performed on the magnetic ground state of Eu. It will be very interesting to determine the changes in the Fermi surface induced by the magnetic ordering since this will be directly proportional to the conduction-4f electrons' interaction.

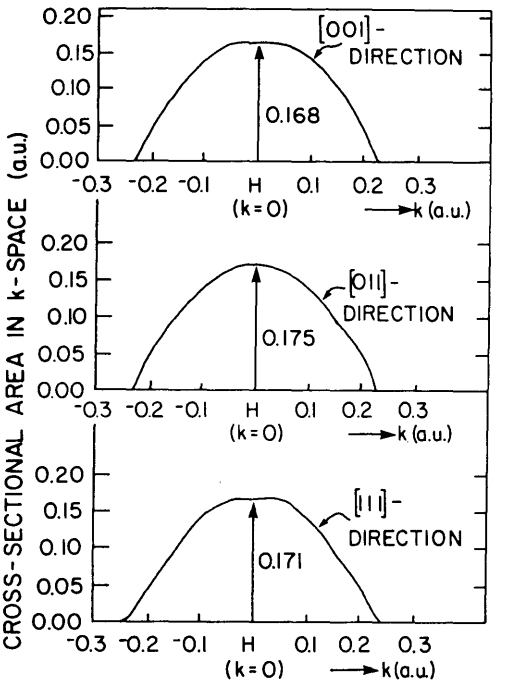

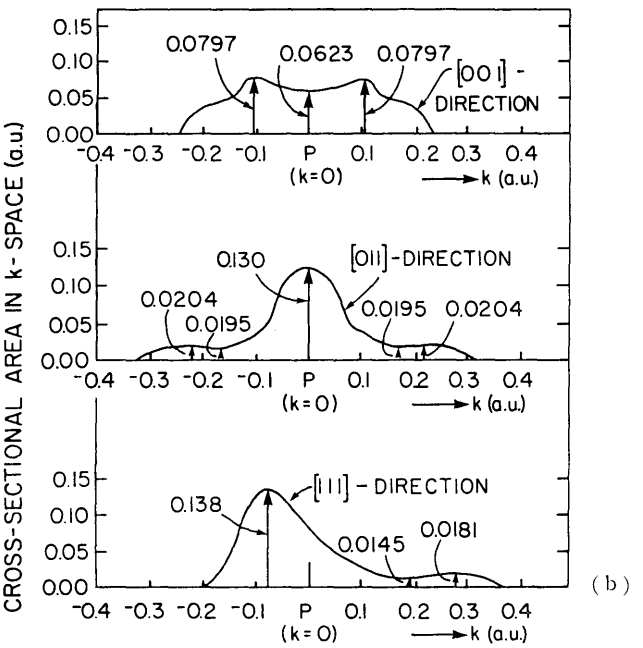

Figure 7. Cross-section areas of our Fermi surface perpendicular to [001]-, [011]- and [111]-directions. (a) Electron Fermi surface. (b) Hole Fermi surface.

Table 1. Extremal cross-section areas of the electron- and the hole-Fermi surfaces and the corresponding dHvA-frequencies.

Fermi surface	Orbit (Ref. 2)	Magnetic field direction	Extremal cross-section in $\boldsymbol{k}$-space (a.u.)	dHvA-frequency (10^6 Gauss)
Bumpy sphere	ε	[001]	0.168 (max)	63.0
(electron)	ε	[011]	0.175 (max)	65.4
		[111]	0.171 (max)	64.0
Tetracube		[001]	0.0797 (max)	29.8
(hole)	δ	[001]	0.0623 (min)	23.3
		[011]	0.0204 (max)	7.63
		[011]	0.0195 (min)	7.29
	γ	[011]	0.130 (max)	48.6
	β	[111]	0.0181 (max)	6.76
	α	[111]	0.0145 (min)	5.43
		[111]	0.138 (max)	51.8

§6. Discussions

The rare-earth metal europium is one of the heavier elements in the periodic table, and therefore, of course, relativistic effects might be important. As we are interested mainly in the Fermi surface, we consider first its effect on the Fermi surface.

In non-relativistic calculations, the F_3-band on the F-axis (from P- to H-points) has a two-fold degeneracy, and since the F_3-band passes through the Fermi energy, the electron- and the hole-parts of the Fermi surface touch each other on the F-axis. Now, if we consider the relativistic effect on spin-orbit splitting, then the double degenerate F_3-state will make a slight separation into two non-degenerate states, as AL have shown in their Fig. 3. If we assume, for simplicity, that the relativistic effects might cause the same small separation to right- and left-side on the F-axis at E_F in Fig. 4 (a), then the electron Fermi surface will become more spherical, since the "bumpy sphere" has eight small mounds in the eight $[\pm 1, \pm 1, \pm 1]$-directions. Then, the electron Fermi surface would become even less effective in the "nesting".

Next, as discussed in Sec. 4, the first peak of interband optical conductivity by Endriz and Spicer[7] occurs at about 1.3 eV, and the corresponding energy difference of N_2 and N_1 in the present SCF-non-relativistic value is 1.5_2 eV. Only for this peak, was there a small discrepancy between the experiment and the calculation. Now, we would like to consider if this error could be reduced by taking into account relativistic effects. As was mentioned earlier, AL have made a relativistic calculation. According to their result (Fig. 3 of Ref. 3), the N_2 and the N_1' states are rather close to each other, and the transitions corresponding to $N_1 \rightarrow N_2$ and $N_1 \rightarrow N_1'$ would give photon energies of about 1.9 eV and 2.0 eV, respectively, both of which are located about in the middle between the first and the second peaks of the experiment.

As we pointed out in our previous paper[6], the relativistic enhancement is very important for the isomer shift on Eu^{151}-nucleus.[11] In spite of the neglect of the important relativistic effects, our present self-consistent band structure gives excellent agreement with the optical experiments, and moreover, our Fermi surfaces exhibit the nesting feature expected to explain helical magnetic moment arrangement. Therefore, we suppose that our present SCF-calculation might not be much affected by inclusion of the relativistic effects, at least, qualitatively. Finally, it will be very interesting to be reflected Fermi surface by the effects of spin polarization and the antiferromagnetic ordering as well as the sd-f hybridization according to $T \rightarrow 0$.[12]

Acknowledgments

The authors would like to express their hearty gratitude to Professor Bruce N. Harmon of Ames Laboratory, Iowa State University for his kind advice and helpful discussions. They also wish to thank Dr. S. Auluck of the University of Roorkee, India (now at Ames Laboratory) for his kind advice. Thanks are also due to Professor A. Yanase of University of Osaka Prefecture for his kind assistance with the author's computer programs. The Ames laboratory is operated for the U.S. Department of Energy by Iowa State University under contract No. W-7405-Eng-82. This work was supported by the Director for Energy Research, Office of Basic Energy Sciences.

REFERENCES

[1] N. G. Nereson, C. E. Olsen and G. P. Arnold: Phys. Rev. **135,** A176 (1964).
[2] A. J. Freeman and J. O. Dimmock: Bull. Amer. Phys. Soc. **11,** 216 (1966).
[3] O. K. Andersen and T. L. Loucks: Phys. Rev. **167,** 551 (1968).
[4] S.-I. Kobayasi, M. Fukuchi and S. Nagai: Solid State Commun. **20,** 589 (1976).
[5] M. Matsumoto, I. Shibata, Y. Sakizi, M. Fukuchi and S.-I. Kobayasi: J. Phys. Soc. Jpn. **49,** 1030 (1980).
[6] M. Matsumoto, M. Fukuchi, Y. Sakizi and S.-I. Kobayasi: J. Phys. F: Metal Physics **13,** 1457 (1983).
[7] J. G. Endriz and W. E. Spicer: Phys. Rev. **B2,** 1466 (1970).
[8] F. Herman and S. Skillman: *Atomic Structure Calculations* (Prentice-Hall, Inc. New York, 1963).
[9] S.-I. Kobayasi, M. Fukuchi and S. Nagai: Solid State Commun. **13,** 727 (1973).
[10] Private communications by Prof. N. Mori, who informed us kindly the importance of the exchange splitting due to the core magnetic moments.
[11] T. Asada and K. Terakura: *Technical Report of ISSP* **A1241,** 1 (1982).
[12] S.-I. Kobayasi, Y. Sakizi, M. Fukuchi and M. Matsumoto: J. Less-Common Met. **94,** 173 (1983).